PHYSICS

Search for exotic parity-violation interactions with quantum spin amplifiers

Yuanhong Wang[1,2]†, Ying Huang[1,2]†, Chang Guo[1,2], Min Jiang[1,2]*, Xiang Kang[1,2], Haowen Su[1,2], Yushu Qin[1,2], Wei Ji[3,4], Dongdong Hu[5], Xinhua Peng[1,2]*, Dmitry Budker[3,4,6]

Quantum sensing provides sensitive tabletop tools to search for exotic spin-dependent interactions beyond the standard model, which have attracted great attention in theories and experiments. Here, we develop a technique based on Spin Amplifier for Particle PHysIcs REsearch (SAPPHIRE) to resonantly search for exotic interactions, specifically parity-odd spin-spin interactions. The present technique effectively amplifies exotic interaction fields by a factor of about 200 while being insensitive to spurious magnetic fields. Our studies, using such a quantum amplification technique, explore the parity-violation interactions mediated by a new vector boson in the challenging parameter space (force range between 3 mm and 1 km) and set the most stringent constraints on axial-vector electron-neutron couplings, substantially improving previous limits by five orders of magnitude. Moreover, our constraints on axial-vector couplings between nucleons reach into a hitherto unexplored parameter space. The present constraints complement the existing astrophysical and laboratory studies on potential standard model extensions.

INTRODUCTION

Numerous theories have predicted the existence of exotic interactions beyond the standard model that are distinct from the four known interactions (*1*, *2*). These exotic interactions were extensively predicted to be mediated by hypothetical spin-0 bosons such as axions and axion-like particles (*3*, *4*), whose existence may explain many central puzzles in physics, including the strong charge-parity problem (*3*, *4*) and the nature of dark matter (*5*, *6*). Subsequently, the interaction mediators were further extended to other new gauge bosons such as massive spin-1 bosons and paraphotons (*2*), resulting in 16 types of potentials under the frame of quantum field theory. A series of astrophysical and laboratory searches are presented to constrain such exotic interactions (*7*, *8*). Since Lee and Yang (*9*) first discussed the use of gravitational equivalence tests (Eötvös-type experiments) to constrain a long-range interaction, recent progress in exploring a broad range of exotic interactions has been enabled by advances in precision techniques (*10*–*21*).

After parity violation was discovered in β decay of ^{60}Co (*22*), various searches for parity violation are performed, including different parity nonconservation tests (*7*, *23*–*25*) and static electric dipole moment searching experiments [see a recent review (*26*) and the references therein]. The manifestation of the parity-violation nature of exotic interactions kindles broad interests in the search for parity-odd interactions, as the study on such exotic interactions has expanded the area of parity-violation research, which could be a harbinger of potential new physics effects beyond the standard model expectations. In the present study, we investigate the parity-odd spin-spin (POSS) interaction induced by the exchange of hypothetical spin-1 Z' bosons. Because of the potential loopholes left by astrophysical observations on the constraints of this interaction (*2*, *27*), it would be valuable to perform direct tests with tabletop experiments. Laboratory searches for the POSS interaction provide an important way for studying the Z' bosons fundamental physics (*2*). However, the Z'-mediated POSS interaction corresponding to V_{11} has been studied less extensively (*15*, *19*, *23*). In particular, it remains challenging to extract the sought-after signal at short (meter scale and shorter) distances due to interference from usual magnetic interactions.

In this work, we report on new results of the "Spin Amplifier for Particle PHysIcs REsearch (SAPPHIRE)" project, which consists of a series of spin amplifier–based experiments to search for exotic particles and interactions (*5*, *10*, *11*). Specifically, a quantum spin amplification technique based on the Xe-Rb system (*5*, *28*) is used to search for the POSS interaction mediated by spin-1 Z' bosons. Our technique takes advantage of the resonant quantum coupling to enhance the signal due to the pseudo-magnetic field, resulting from the exotic interactions by a factor of about 200. By greatly suppressing spurious external magnetic field, the present experiment fills the gap of searching for the POSS interaction between electrons and neutrons in the force range of 3×10^{-3} to 3×10^{3} m and sets the most stringent limits on the axial-vector electron-neutron coupling, substantially improving current laboratory limits on $g_A^e g_V^n$ by up to five orders of magnitude (*23*). Moreover, considering the contribution of nuclear spins in the polarized ^{87}Rb, the POSS couplings $g_V^n g_A^p$ and $g_A^n g_V^p$ between nucleons are tightly constrained. In addition, experimental searches for the POSS interaction at short distance enable the study of spin-1 Z' bosons in the mass range of 10^{-10} to 10^{-4} eV, while Z' bosons with mass less than 3.9×10^{-11} eV may be excluded by the analysis of the superradiant phenomena of spinning astrophysical black holes (*29*).

[1]CAS Key Laboratory of Microscale Magnetic Resonance and School of Physical Sciences, University of Science and Technology of China, Hefei 230026, Anhui, China. [2]CAS Center for Excellence in Quantum Information and Quantum Physics, University of Science and Technology of China, Hefei 230026, Anhui, China. [3]Helmholtz-Institut, GSI Helmholtzzentrum für Schwerionenforschung, Mainz 55128, Germany. [4]Johannes Gutenberg University, Mainz 55128, Germany. [5]State Key Laboratory of Particle Detection and Electronics, University of Science and Technology of China, Hefei 230026, Anhui, China. [6]Department of Physics, University of California, Berkeley, Berkeley, CA 94720-7300, USA.
*Corresponding author. Email: dxjm@ustc.edu.cn (M.J.); xhpeng@ustc.edu.cn (X.P.)
†These authors contributed equally to this work.

RESULTS

Principle

We focus on the exotic POSS interaction between electrons and neutrons (Fig. 1), whose corresponding potential following the notation in (*2*, *30*) is given as ($\hbar = c = 1$)

$$V_{11} = -f_{11}[(\hat{\sigma}_n \times \hat{\sigma}_e)\cdot \hat{r}]\left(\frac{1}{\lambda r} + \frac{1}{r^2}\right)\frac{e^{-r/\lambda}}{4\pi m_e} \quad (1)$$

where $\hat{\sigma}_e$ ($\hat{\sigma}_n$) is the total spin operator of electron (neutron), $\hat{r}$ is the unit vector directed from electrons to neutrons, r is the distance between them, λ is the force range, and f_{11} is the dimensionless coupling constant. The potential can be generated by the exchange of an ultralight spin-1 boson Z' whose mass $m_{Z'} = \lambda^{-1}$ determines the force range of the interaction (*2*, *30*). The exotic POSS interaction would exert a torque on the nuclear spin of the spin sensor, generating a pseudo-magnetic field $\mathbf{B}_{11} \propto -f_{11}\cdot(\hat{\sigma}_e \times \hat{r})$ on the spin sensor. The specific form of the pseudo-magnetic field is provided in Methods. Note that the exotic field $\mathbf{B}_{11}$ acted on the mirror symmetrical spin sensor is in the opposite direction to the one before parity transformation (Fig. 1), illustrating that the parity of the V_{11} interaction is broken.

Experimental searches for exotic spin-spin interactions are typically performed by positioning two polarized objects in close proximity to each other, with one acting as a sensitive magnetic detector ("spin sensor") to measure the exotic field produced by the other polarized object ("spin source"). Objects with large polarization number density are preferentially chosen as the spin source and placed close enough to the spin sensor for maximizing exotic signals. In our experiment, the spin sensor uses polarized neutron spins of isotopically enriched polarized ^{129}Xe gas, and the spin source uses polarized electron spins of ^{87}Rb atoms.

The experimental setup is shown in Fig. 2A. A 0.58-cm^3 cubic glass cell containing polarized ^{87}Rb vapor with 600 torr of N_2 buffer gas is used as the spin source and is positioned 50.7 mm above the center of the spin-sensor vapor cell. The spin-source vapor cell is heated to 180°C to obtain ^{87}Rb number density (≈4.0 × 10^{14} cm^{-3}). A laser beam generated with a tapered amplifier system with a power of 0.34 W is tuned to the D1 transition of ^{87}Rb and delivered to the spin-source vapor cell along $\hat{z}$ with a single-mode fiber. The laser beam is circularly polarized and expanded to pump all the ^{87}Rb in the spin-source cell to an average electron polarization of >0.9, and the corresponding number of polarized ^{87}Rb electron spins is about (2.1 ± 0.2) × 10^{14}. Here, the electron polarization along $\hat{z}$ defined as $P_z = 2\langle S_z\rangle$ is determined by numerical calculations, where all the required parameters (such as ^{87}Rb number density and pump laser power) are experimentally calibrated (see section SIII.A for details). The uncertainty of the electron polarization is estimated from the uncertainties of the relevant parameters. The spin sensor and the spin source are both enclosed within a single-layer magnetic shield.

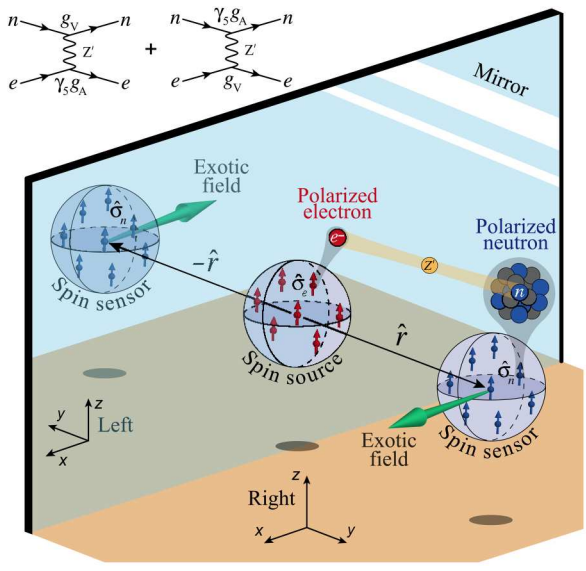

Fig. 1. Illustration of POSS interaction. The exotic interaction between electrons and neutrons involving the exchange of Z' bosons can be described by the Feynman diagrams (*2*). As a parity-odd interaction, the induced exotic pseudo-magnetic field changes sign under a parity transformation as shown in the mirror.

Quantum amplification technique

A quantum spin amplifier (*5*, *28*) is introduced to resonantly amplify the effect of the exotic field $\mathbf{B}_{11}$. The spin amplifier uses spatially overlapping hyperpolarized long-lived ^{129}Xe nuclear spins and optically pumped polarized ^{87}Rb spins (section SII). The ^{129}Xe spins are polarized by spin-exchange collisions with polarized ^{87}Rb spins (*5*, *28*). A constant field $B_0\hat{z}$ is applied in the sensor, along with an oscillatory transverse field $\mathbf{B}_{ac}$ to be measured. When the oscillation frequency of $\mathbf{B}_{ac}$ matches the ^{129}Xe Larmor frequency, the polarized ^{129}Xe spins are tilted away from their polarization axis and generate a transverse oscillatory magnetization. Because of Fermi contact interactions (*5*, *28*), an effective field $\mathbf{B}^n_{eff}$ generated by the transverse magnetization is read out by the embedded ^{87}Rb spins that act as an in situ magnetometer. We find that the ^{129}Xe spins can act as a quantum preamplifier, which converts the external resonant field into an amplified field $|\mathbf{B}^n_{eff}| \gg |\mathbf{B}_{ac}|$ without introducing additional noise.

The amplification effect can be quantitatively described by introducing an amplification factor (*5*, *28*)

$$\eta = |\mathbf{B}^n_{eff}| / |\mathbf{B}_{ac}| = \frac{4\pi}{3}\kappa_0\gamma_N M_z^N T_2^N \quad (2)$$

where $\kappa_0 \approx 540$ is the Fermi contact enhancement factor, γ_N is the gyromagnetic ratio of ^{129}Xe nucleus, and M_z^N and T_2^N are the initial longitudinal magnetization and the transverse relaxation time of ^{129}Xe, respectively. For the ^{129}Xe-^{87}Rb system used in this work, the amplification factor is measured to be $\eta \approx 187.4$. This shows that the spin amplifier can enhance the effect of the exotic pseudo-magnetic field by more than two orders of magnitude.

Similar resonant techniques based on nuclear magnetic resonance have been recently introduced to search for exotic interactions (*13*, *14*, *31*), and most of their experimental demonstrations are still ongoing. Similar to the quantum spin amplifier, these resonant techniques measure exotic fields through measuring the response of nuclear spins with an auxiliary magnetometer. In contrast, ^{87}Rb atoms in the spin amplifier act as an embedded magnetometer, enabling in situ measurement and continuous polarization of the ^{129}Xe atoms. A notable advantage offered by in situ measurements is the enhancement of the nuclear resonance signals due to the large Fermi contact amplification factor. In addition, because ^{129}Xe nuclear spins are polarized continuously by

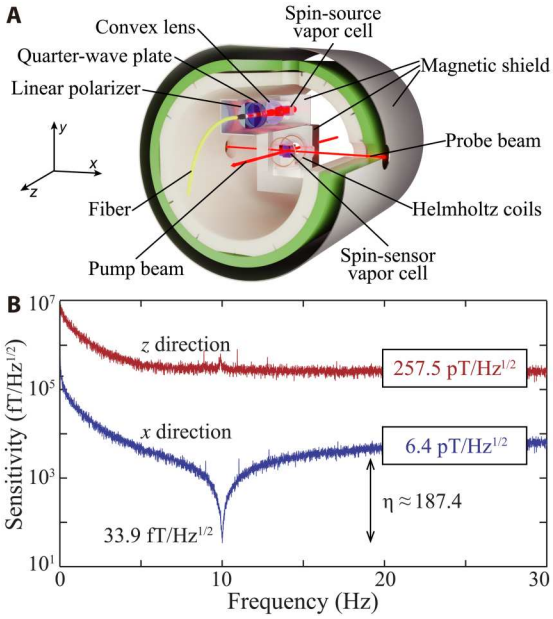

Fig. 2. Spin amplification setup and magnetic field sensitivity. (**A**) The ^{87}Rb atoms (the spin source) contained in a vapor cell with N_2 buffer gas are polarized with a circularly polarized laser beam. The spin-sensor cell containing enriched ^{129}Xe, buffer gas N_2, and a droplet of ^{87}Rb is placed below the spin source. A circularly polarized beam along $\hat{z}$ and a linearly polarized beam along $\hat{x}$ are used to respectively pump and probe the spin sensor. See section SI for more details on the experimental setup. (**B**) The sensitivity of the spin amplifier along $\hat{x}$ is measured to be 33.9 fT/Hz$^{1/2}$ at the resonance frequency and 6.4 pT/Hz$^{1/2}$ off resonance. In contrast, the magnetic sensitivity along $\hat{z}$ is only 257.5 pT/Hz$^{1/2}$.

spin-exchange collisions with polarized ^{87}Rb, the spin amplifier can search for exotic fields with a 100% duty cycle. Because of these unique advantages, the spin amplifier is suitable for ultrasensitive continuous wave detection of exotic interactions (*10*, *11*).

We calibrate the magnetic sensitivity of the quantum spin amplifier, which is important for determining the sensitivity to the POSS interaction. By scanning the frequency of the applied oscillatory field, we obtain the frequency dependence of the sensitivity to magnetic fields along $\hat{x}$ and $\hat{z}$, respectively depicted in Fig. 2B. The ^{129}Xe Larmor frequency is tuned to $\nu_0 \approx 10.0$ Hz by setting the constant magnetic field $B_0\hat{z}$ at 847 nT to avoid low-frequency noise. The optimal magnetic sensitivity is 33.9 fT/H$^{1/2}$ at the resonance frequency, with the oscillatory field applied along $\hat{x}$, while the off-resonance sensitivity is only 6.4 pT/Hz$^{1/2}$. The spin amplifier is only sensitive to a transverse oscillatory field, because fields along the polarization axis cannot induce a measurable transverse magnetization. As a result, the residual sensitivity to $\hat{z}$ fields (owing to the Rb magnetometer) of (≈257.5 pT/Hz$^{1/2}$) is about two orders of magnitude worse than that to $\hat{x}$ fields. Taking advantage of the sensitivity anisotropy of the spin amplifier, it is possible to distinguish spurious magnetic fields from the pseudo-magnetic field.

To resonantly search for the POSS interaction, we modulate the polarization of the spin source, thus modulating the pseudo-magnetic field $\mathbf{B}_{11}$. The exotic signal is modulated by periodically blocking the pump laser beam, with a 50% duty cycle, with an optical chopper. Once the chopping frequency matches the resonance frequency (i.e., $\nu \approx \nu_0 \approx 10.0$ Hz), the spin amplifier enables to resonantly search for the exotic field with a sensitivity improvement of about 200 (see Methods for details).

Unlike our recent work (*10*) using an unpolarized source for detecting spin-mass velocity-dependent interactions, the polarized spin source in this work inevitably generates an ordinary magnetic field in addition to the exotic field. The existence of these magnetic fields poses a large challenge for spin-spin interaction searches. Large-size magnetic shields (*15*) or long-range detection (*19*) was usually used in the previous search experiments, where the spin source was thus far from the spin sensor. This sets a bottleneck for improving sensitivity to the exotic signal in short force ranges (~1 cm) due to the exponential falloff of the signal. As a result, most experimental studies on spin-spin interactions have focused on meter-scale searches, corresponding to mediator masses less than 10^{-4} meV. In our case, a notable dipole magnetic field of about 1.5 pT would be produced by the polarized ^{87}Rb spins acting on the spin sensor if the source and the sensor were not enclosed in additional shielding. We arrange the spin source directly above the spin sensor (see Fig. 2A), where the dipole magnetic field is mostly oriented along the insensitive axis of the spin amplifier. However, because the spin source is not ideally positioned above the spin sensor and volumetric effect of the spin source cannot be ignored, there is still a transverse dipole magnetic field of about 0.27 pT. Therefore, two single-layer μ-metal shieldings are used for both the source and the sensor with the total combined shielding factor experimentally determined to be about 10^4. The component of the magnetic field experienced by the spin sensor along the sensitive directions is estimated to be about 10 aT (see section SIV for details), which can be negligible with respect to the 0.12-fT magnetic field detectable by the spin amplifier for 24 hours of operation. Taking advantage of sensitivity anisotropy and small-size magnetic shields, the magnetic field is suppressed by about five orders of magnitude in total, enabling to test the POSS interaction at short distance, down to about the millimeter range.

Table 1. Summary of calibrated parameters and systematic errors. The corrections to f_{11} for $\lambda = 0.1$ m are listed.

Parameter	Value	$\Delta f_{11}(\times 10^{-22})$
Position of spin source x (mm)	−1.41 ± 0.40	<0.01
Position of spin source y (mm)	50.67 ± 0.71	±0.07
Position of spin source z (mm)	3.19 ± 0.01	<0.01
Number of polarized Rb	(2.14 ± 0.24) × 10^{14}	$^{-0.17}_{+0.20}$
Phase delay ϕ_a (°)	13.20 ± 0.54	$^{+0.71}_{-0.45}$
Calibrated constant α (V/nT)	$1.99^{<0.01}_{-0.17}$	$^{<0.01}_{+0.19}$
Final $f_{11}(\times 10^{-22})$	2.12	±0.77 (syst)
($\lambda = 0.1$ m)		±5.78 (stat)

New constraints on parity-odd interactions

The experimental search for the POSS interaction consists in calibration experiments and search experiments. We perform calibration experiments to determine the required parameters. Calibrated parameters and corresponding values are summarized in the first and second columns of Table 1, respectively. Calibrated parameters are used to obtain a reference signal of the pseudo-magnetic field for

subsequent data analysis. During search experiments, data are collected in records of 1 hour. The total duration of search data is 24 hours, and the weakest external resonant (pseudo-)magnetic field being able to be sensed by the spin amplifier is obtained as $B_{24h} \approx 0.12$ fT.

Using the search data, we can obtain the coupling strength for a total of 24 hours as $f_{11} \approx (2.1 \pm 5.\,8_{stat}) \times 10^{-22}$ for the force range $\lambda = 0.1$ m, as shown in Table 1. The corresponding systematic errors caused by the uncertainty of each parameter are also listed in the third column, in which the major systematic error comes from the phase delay of the spin amplifier. By combining all the systematic errors in quadrature, which are assumed to be independent of each other, the overall systematic uncertainty is derived as $\pm 0.77 \times 10^{-22}$. Accordingly, for the force range $\lambda = 0.1$ m, we quote the final coupling strength as $f_{11} \approx (2.1 \pm 5.\,8_{stat} \pm 0.\,8_{syst}) \times 10^{-22}$, which means that no POSS interaction is detected in our experiment. The final constraint for $\lambda = 0.1$ m can be determined as 1.5×10^{-21} at the 95% confidence level (see section SV for more details about data analysis). By varying the force range λ and repeating the above process, constraints for the entire explored force range are obtained. We can constrain the gauge coupling of Z' bosons as mediators of the POSS interaction (*2*), whose existence arises in numerous standard model extensions such as supersymmetric theories and general hidden portal models (*32*). The POSS interaction can be induced by exchange of a Z' boson following the effective Lagrangian as depicted by the Feynman diagrams in Fig. 1 (*2*, *30*)

$$\mathcal{L}_{Z'} = Z'_{\mu} \sum_{\psi=e,n} [\overline{\psi}\gamma^{\mu}(g_V^{\psi} + g_A^{\psi}\gamma_5)\psi] \tag{3}$$

where ψ denotes fermion field (electron or neutron), $g_A^{\psi}(g_V^{\psi})$ stands for the axial (vector) coupling to the fermion ψ, and γ^{μ} and $\gamma_5 = i\gamma^0\gamma^1\gamma^2\gamma^3$ are Dirac matrices. The dimensionless coefficient f_{11} related to couplings constants $g_{A,V}^{\psi}$ following the notation of equation (5.29) in (*2*) is given as

$$f_{11}^{en} = \frac{1}{2} g_V^e g_A^n + \frac{m_e}{2m_n} g_A^e g_V^n \tag{4}$$

where ^{129}Xe and ^{87}Rb respectively contribute the neutrons and electrons in our experiment. Here, the contribution of nucleon in ^{87}Rb is ignored (it is discussed below). The product of vector and axial coupling constant $g_V g_A$ can only be directly constrained by two exotic interactions V_{11} and V_{12+13} (*30*). However, V_{12+13} as a spin-mass interaction constrains the coupling constant between unpolarized fermions and the electron spin $g_A^e g_V^N$. Here, N denotes unpolarized nucleus. In contrast, the POSS interaction V_{11} can directly constrain $g_V g_A$ between two fermion spins.

Figure 3A shows the experimental constraints on the POSS couplings between electrons and neutrons. For the force range $\lambda > 10^3$ m, the most stringent constraints were set by Hunter *et al.* (*19*) as shown with the black line, where the polarized electrons of the Earth were used as the spin source. However, the work did not constrain the couplings for the force range $\lambda < 10^3$ m, as their limits are exponentially suppressed at short distances because the relative contribution to polarized electrons from the Earth's outermost crust is only 2% (*19*). For the force range $\lambda < 3 \times 10^{-3}$ m, the most stringent limits on $g_A^e g_V^n$ (blue line) were set from atomic parity-violation tests by detecting the induced electric dipole transition (*23*). Our searches rely on centimeter-scale detection technique, bridging the gap between atomic-scale and Earth-scale experiments. In consequence, our result yields the most stringent constraints for 3×10^{-3} m $< \lambda <$ 10^3 m (red solid line), improving over previous limits by up to five orders of magnitudes.

Our experiment can also constrain the POSS coupling constants between nucleons. We consider valence protons within the Rb nuclei in the spin source. The valence proton is nearly fully polarized (~90%) due to the high polarization of ^{87}Rb. The proton-neutron coupling strength f_{11} can be redefined as

$$f_{11}^{np} = \frac{m_e}{2m_p} g_A^n g_V^p + \frac{m_e}{2m_n} g_V^n g_A^p \tag{5}$$

Our work also provides new experimental limits on $g_A^n g_V^p$ (and $g_V^n g_A^p$), as shown by the red solid line in Fig. 3B. Our work sets the best constraints on the POSS coupling and reaches into the hitherto unexplored parameter space to test parity-odd interaction between nucleons.

DISCUSSION

Astrophysical and cosmological observations can usually be used to constrain the coupling strength between hypothetical bosons and standard model particles. The coupling constant of spin-0 bosons to electrons and nucleons are tightly constrained by astrophysical limits, such as those from star cooling. It is the opposite for spin-1 exchange interactions, where potential loopholes may exist in the relevant theories (*2*, *27*). As a result, our constraints from laboratory direct search for the spin-1 exchange POSS interaction are the most stringent, where astrophysical limits are relaxed.

There is still room for improvement in the present experiment. We now modulate spin polarization by chopping circularly polarized pump light; if instead we reverse the direction of the circular polarization, then this will yield a gain of a factor of 2 in the exotic field amplitude and, moreover, would allow to better subtract possible systematic effect due to the apparatus imperfections. Such systematics would be further suppressed by adding an additional symmetrically located spin sensor and/or spin source (Fig. 1). Such an arrangement would allow taking full advantage of all possible reversals implied by the form of the POSS interaction (Eq. 7). In addition, searches with longer time than that in the present work would further tighten the limits, where some systematic errors may be eliminated by daily result analysis.

Further improvement in experimental sensitivity to the POSS interactions can be anticipated by replacing the Xe-Rb system in the spin amplifier with a ^{3}He-K system (*5*, *10*, *12*). As seen in Eq. 2, to realize larger amplification, a prerequisite is to achieve long transverse relaxation time and high polarized spin density of noble gas. Specifically, the predicted amplification factor of a ^{3}He-K system can be better than the current one by at least two orders of magnitude (*15*). In addition to the amplification factor, K magnetometers have higher magnetic sensitivity (a few femtotesla/hertz$^{1/2}$) than Rb magnetometers (*15*). In this case, the final magnetic sensitivity of the spin sensor is limited by the Johnson-Nyquist noise caused by small μ-metal shielding, which is estimated to be at the level of 10 fT/Hz$^{1/2}$. However, using low electrical conductivity manganese zinc ferrites would suppress the magnetic noise (*33*). Moreover, the use of gradient detection can further eliminate the magnetic noise by nearly two orders of magnitude without suppressing the

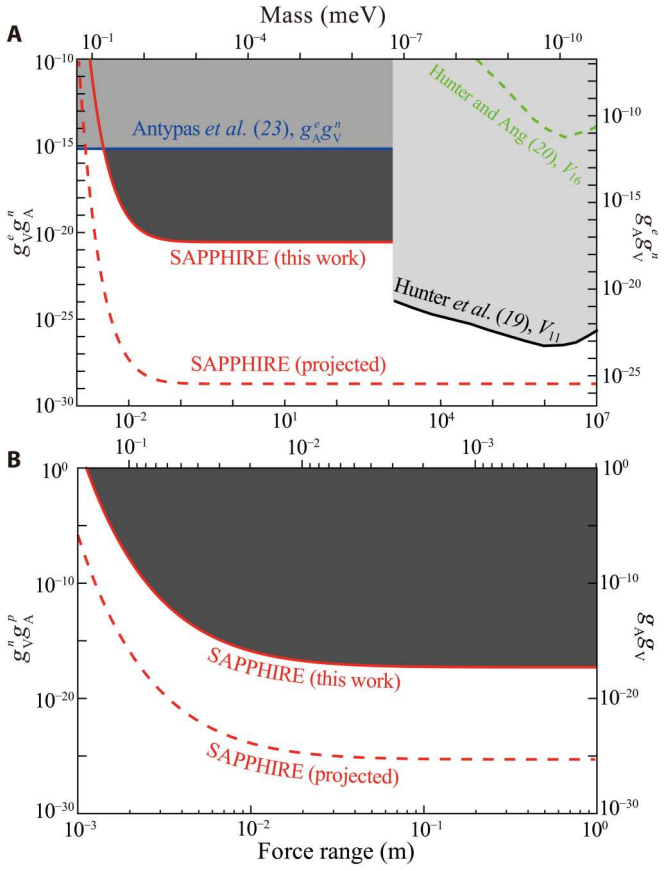

Fig. 3. Constraints on POSS coupling strengths. After a 24-hour search, the weakest magnetic field able to be sensed by the spin sensor is 0.12 fT. The red solid line represents the experimental limits at the 95% confidence level as a function of the force range λ and the boson mass (top axis). The red dashed line is projected sensitivity obtained by combining the proposal ^{3}He-K spin amplifier with a highly polarized solid-state spin source. (**A**) The vertical axes on the left and right represent the constraints on $g_V^e g_A^n$ and $g_A^e g_V^n$, respectively. The black solid (*19*) and green dashed (*20*) lines indicate the constraints from the measurement of V_{11} and V_{16}, respectively, using polarized electrons in the Earth. The blue line stands for the constraints on $g_A^e g_V^n$ from combining results of the Cs and Yb parity-violation experiments (*23*, *39*). (**B**) The vertical axis on the left and right represent the limits on $g_V^n g_A^p$ and $g_A^n g_V^p$, respectively.

exponential distance–dependent POSS interaction (*34*). Overall, the projected magnetic sensitivity of the spin sensor can be improved by about four orders of magnitude over the current spin amplifier.

The number density of polarized spins in the source can be greatly increased by using solid-state spin sources, such as nitrogen-vacancy centers in diamonds (*35*, *36*) and pentacene-doped terphenyl crystal (*37*, *38*). Near-unity spin polarization can be realized with optical pumping. For example, a crystal of *p*-terphenyl doped with 0.1 mole percent (mol %) fully deuterated pentacene can be a good candidate for high-polarization spin sources, with polarized-electron density reaching $\sim 1.5 \times 10^{18}$ cm^{-3} under optical pumping (*37*). The high nucleon polarization of synthesized deuterated *p*-terphenyl-2′,3′,5′,6′-d_4 (~34%) can be created by dynamic nuclear polarization at room temperature, which transfers the polarization from the electrons of deuterated pentacene 0.05 mol% to the protons of terphenyl, with the total number of polarized protons achieved exceeding 3×10^{18} (*38*). Overall, using optically pumped pentacene-doped terphenyl crystals, one could increase the strength of exotic field by about four orders of magnitude. Combining the enhanced spin amplifier based on ^{3}He-K system discussed above and highly polarized solid-state spin sources, the projected sensitivity is better than our present limits by about eight orders of magnitude (red dashed lines in Fig. 3). Over a wide force range, the projected sensitivity would improve on the existing bounds, including the limits from the Earth-geoelectron experiments (*19*, *20*).

In this work, we have reported new constraints on $g_V g_A$ between electrons and neutrons by exploring the exotic POSS interaction with a spin amplifier, improving previous limits by up to five orders of magnitude. Moreover, by considering valence protons of the Rb nuclei within the spin source, new constraints are placed on the proton-neutron axial-vector coupling. Further improvement in experimental sensitivity can be anticipated by replacing the ^{129}Xe-Rb system in the spin amplifier with a ^{3}He-K system and using solid-state spin sources. In this case, the experimental sensitivity to the POSS interaction can be further improved by eight orders of magnitude. This makes it possible to discover new physics on Z' bosons with the ultrasensitive SAPPHIRE experiments.

METHODS

Pseudo-magnetic field

The exotic POSS interaction generates a pseudo-magnetic field acting on the spin-sensor nuclear spins. To obtain the specific form of the pseudo-magnetic field, we first rewrite the POSS potential V_{11} as

$$V_{11} = -f_{11}[\hat{\sigma}_n \cdot (\hat{\sigma}_e \times \hat{r})]\left(\frac{1}{\lambda r} + \frac{1}{r^2}\right)\frac{e^{-r/\lambda}}{4\pi m_e} \quad (6)$$

By analogy with the Zeeman Hamiltonian $\hat{H} = -\mu \cdot \mathbf{B}$, we obtain the form of the pseudo-magnetic field generated by the potential V_{11} as

$$\mathbf{B}_{11} = f_{11}(\hat{\sigma}_e \times \hat{r})\left(\frac{1}{\lambda r} + \frac{1}{r^2}\right)\frac{e^{-r/\lambda}}{4\pi \mu_{Xe} m_e} \quad (7)$$

where $\mu_{Xe} = \mu_{Xe}\hat{\sigma}_n$. In our experiment, the spin-source electron spins are polarized along the $\hat{z}$ axis, and the spin source is positioned directly above the spin sensor along $\hat{y}$ (Fig. 2A), so the exotic field is primarily along $\hat{x}$. However, because of the close proximity of the spin sensor and the spin source, the volume shape and polarization gradient of the spin source cannot be ignored. Considering all the spins and their spatial distribution in the spin source, the pseudo-magnetic field is obtained by integrating over the volume of the spin source

$$\mathbf{B}_{11} = \int_V \rho(\boldsymbol{r}) f_{11}(\hat{\sigma}_e \times \hat{r})\left(\frac{1}{\lambda r} + \frac{1}{r^2}\right)\frac{e^{-r/\lambda}}{4\pi \mu_{Xe} m_e} d\boldsymbol{r} \quad (8)$$

where V represents the integration volume of the spin-source cell and $\rho(\boldsymbol{r})$ is the number density of the polarized electron spins. The calibration of $\rho(\boldsymbol{r})$ is provided in section SIII.A.

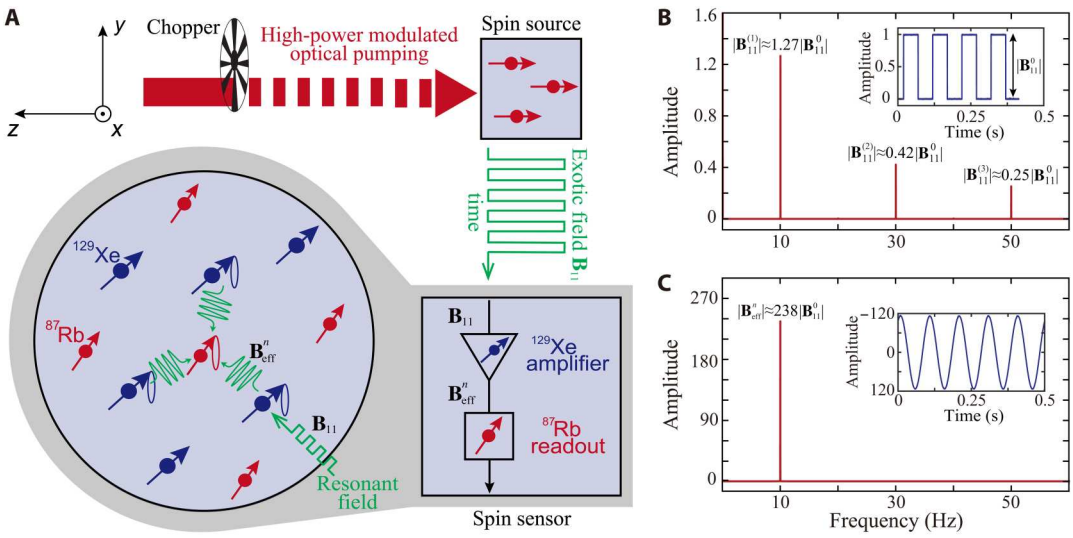

Fig. 4. Demonstration of resonance-sensitive search for exotic signal based on spin amplifier. (**A**) Under a high-power (>0.34 W) modulated optical pumping along $\hat{z}$, the spin source generates a $\hat{x}$-directed square-wave pseudo-magnetic field on the spin sensor with 50% duty cycle at a frequency of $\nu \approx 10.0$ Hz. The exotic signal $\mathbf{B}_{11}$ is enhanced by the ^{129}Xe atoms, yielding an effective field $\boldsymbol{B}^{n}_{\mathrm{eff}}$ read out by ^{87}Rb atoms. (**B**) Ratios of the peak-to-peak amplitude of square-wave's *N*th harmonic relative to the amplitude of original signal $|\,\mathbf{B}^{0}_{11}\,|$. Right top inset: Experimental measured time-domain square-wave signal of simulated exotic field $\mathbf{B}_{11}$. (**C**) Experimental response in frequency domain of the spin amplifier to the square-wave magnetic field. Only the first harmonic of the input exotic signal $\mathbf{B}^{(1)}_{11}$ can be amplified and detected.

Modulation technique and resonant search

To resonantly search for the exotic POSS interaction, we modulate the pseudo-magnetic field $\mathbf{B}_{11}$ by modulating the polarization of the spin source. As shown in Fig. 4A, the exotic signal is modulated by periodically blocking the pump laser beam, with a 50% duty cycle, with an optical chopper. The modulated pseudo-magnetic field as a function of time can be represented as

$$\begin{aligned}\mathbf{B}_{11}(t) &= \mathbf{B}^{0}_{11}\cdot\left\{\frac{1}{2}+\frac{\mathscr{S}[\sin(2\pi\nu t+\phi)]}{2}\right\},\\ &= \sum_{N=\mathrm{odd}}\mathbf{B}^{(N)}_{11}\frac{\sin(2\pi N\nu t+\phi_N)}{2}+C\end{aligned} \tag{9}$$

where $\mathbf{B}^{0}_{11}$ is the pseudo-magnetic field produced by the spin source under pumping, $\mathscr{S}$ stands for the signum function, ϕ is the initial phase of the exotic signal, and $|\,\mathbf{B}^{(N)}_{11}\,|=|\,\mathbf{B}^{0}_{11}\,|\cdot 4/(\pi N)$ is the peak-to-peak amplitude of the *N*th harmonic, ϕ_N is the corresponding phase, and $C=\mathbf{B}^{0}_{11}/2$ is the dc component of the signal. Here, we ignore the rising edge and falling edge of the exotic square-wave signals, because the transient of the source polarization, which is faster than the relaxation time of electrons (~1 ms), is much shorter than the pumping period (~100 ms). Once the optical chopping frequency matches the resonance frequency (i.e., $\nu \approx \nu_0 \approx 10.0$ Hz), the spin amplifier enables to resonantly search for the exotic field with a sensitivity improvement of about 200.

We experimentally test the sensitivity of the resonant measurement by applying a square-wave (real) field to the spin amplifier to simulate the modulated exotic field with an amplitude of $|\,\mathbf{B}^{0}_{11}\,|$, whose Fourier transform spectrum contains only odd harmonics (Fig. 4B). As the primary component of simulated exotic fields, the first harmonic with peak-to-peak amplitude of $|\,\mathbf{B}^{(1)}_{11}\,|$ is about 1.27 times larger than the signal $\mathbf{B}^{0}_{11}$. The resonance frequency of spin amplifier is tuned to match the frequency of the modulated field. Only the first harmonic of the field is amplified by the spin sensor, and the effects of other harmonics are negligible (Fig. 4C).

Supplementary Materials

This PDF file includes:

Sections SI to SV
Figs. S1 to S5

REFERENCES AND NOTES

1. J. Moody, F. Wilczek, New macroscopic forces? *Phys. Rev. D* **30**, 130–138 (1984).
2. B. A. Dobrescu, I. Mocioiu, Spin-dependent macroscopic forces from new particle exchange. *J. High Energy Phys.* **2006**, 005 (2006).
3. R. D. Peccei, H. R. Quinn, CP conservation in the presence of pseudoparticles. *Phys. Rev. Lett.* **38**, 1440–1443 (1977).
4. J. E. Kim, G. Carosi, Axions and the strong CP problem. *Rev. Mod. Phys.* **82**, 557–601 (2010).
5. M. Jiang, H. Su, A. Garcon, X. Peng, D. Budker, Search for axion-like dark matter with spin-based amplifiers. *Nat. Phys.* **17**, 1402–1407 (2021).
6. L. D. Duffy, K. Van Bibber, Axions as dark matter particles. *New J. Phys.* **11**, 105008 (2009).
7. M. . S. Safronova, D. Budker, D. De Mille, D. F. Jackson Kimball, A. Derevianko, C. W. Clark, Search for new physics with atoms and molecules. *Rev. Mod. Phys.* **90**, 025008 (2018).
8. D. DeMille, J. M. Doyle, A. O. Sushkov, Probing the frontiers of particle physics with tabletop-scale experiments. *Science* **357**, 990–994 (2017).
9. T. Lee, C.-N. Yang, Conservation of heavy particles and generalized gauge transformations. *Phys. Rev.* **98**, 1501 (1955).
10. H. Su, Y. Wang, M. Jiang, W. Ji, P. Fadeev, D. Hu, X. Peng, D. Budker, Search for exotic spin-dependent interactions with a spin-based amplifier. *Sci. Adv.* **7**, eabi9535 (2021).
11. Y. Wang, H. Su, M. Jiang, Y. Huang, Y. Qin, C. Guo, Z. Wang, D. Hu, W. Ji, P. Fadeev, X. Peng, D. Budker, Limits on axions and axionlike particles within the axion window using a spin-based amplifier. *Phys. Rev. Lett.* **129**, 051801 (2022).
12. W. Ji, Y. Chen, C. Fu, M. Ding, J. Fang, Z. Xiao, K. Wei, H. Yan, New experimental limits on exotic spin-spin-velocity-dependent interactions by using $SmCo_5$ spin sources. *Phys. Rev. Lett.* **121**, 261803 (2018).
13. P.-H. Chu, Y. Kim, I. Savukov, Search for exotic spin-dependent interactions using polarized helium. arXiv: 2002.02495(2020).https://arxiv.org/abs/2002.02495.

14. A. Arvanitaki, A. A. Geraci, Resonantly detecting axion-mediated forces with nuclear magnetic resonance. *Phys. Rev. Lett.* **113**, 161801 (2014).
15. G. Vasilakis, J. Brown, T. Kornack, M. Romalis, Limits on new long range nuclear spin-dependent forces set with a K-^{3}He comagnetometer. *Phys. Rev. Lett.* **103**, 261801 (2009).
16. M. Bulatowicz, R. Griffith, M. Larsen, J. Mirijanian, C. B. Fu, E. Smith, W. M. Snow, H. Yan, T. G. Walker, Laboratory search for a long-range T-odd, P-odd interaction from axionlike particles using dual-species nuclear magnetic resonance with polarized ^{129}Xe and ^{131}Xe gas. *Phys. Rev. Lett.* **111**, 102001 (2013).
17. X. Rong, M. Jiao, J. Geng, B. Zhang, T. Xie, F. Shi, C. K. Duan, Y. F. Cai, J. du, Constraints on a spin-dependent exotic interaction between electrons with single electron spin quantum sensors. *Phys. Rev. Lett.* **121**, 080402 (2018).
18. H. Yan, W. Snow, New limit on possible long-range parity-odd interactions of the neutron from neutron-spin rotation in liquid ^{4}He. *Phys. Rev. Lett.* **110**, 082003 (2013).
19. L. Hunter, J. Gordon, S. Peck, D. Ang, J.-F. Lin, Using the earth as a polarized electron source to search for long-range spin-spin interactions. *Science* **339**, 928–932 (2013).
20. L. Hunter, D. Ang, Using geoelectrons to search for velocity-dependent spin-spin interactions. *Phys. Rev. Lett.* **112**, 091803 (2014).
21. F. M. Piegsa, G. Pignol, Limits on the axial coupling constant of new light bosons. *Phys. Rev. Lett.* **108**, 181801 (2012).
22. C.-S. Wu, E. Ambler, R. W. Hayward, D. D. Hoppes, R. P. Hudson, Experimental test of parity conservation in beta decay. *Phys. Rev.* **105**, 1413–1415 (1957).
23. D. Antypas, A. Fabricant, J. E. Stalnaker, K. Tsigutkin, V. V. Flambaum, D. Budker, Isotopic variation of parity violation in atomic ytterbium. *Nat. Phys.* **15**, 120–123 (2019).
24. V. Dzuba, V. Flambaum, P. Munro-Laylim, Long-range parity-nonconserving electron-nucleon interaction. *Phys. Rev. A* **106**, 012817 (2022).
25. V. Dzuba, V. Flambaum, Y. Stadnik, Probing low-mass vector bosons with parity nonconservation and nuclear anapole moment measurements in atoms and molecules. *Phys. Rev. Lett.* **119**, 223201 (2017).
26. T. Chupp, P. Fierlinger, M. Ramsey-Musolf, J. Singh, Electric dipole moments of atoms, molecules, nuclei, and particles. *Rev. Mod. Phys.* **91**, 015001 (2019).
27. P. Jain, S. Mandal, Evading the astrophysical limits on light pseudoscalars. *Int. J. Mod. Phys. D* **15**, 2095–2103 (2006).
28. M. Jiang, Y. Qin, X. Wang, Y. Wang, H. Su, X. Peng, D. Budker, Floquet spin amplification. *Phys. Rev. Lett.* **128**, 233201 (2022).
29. M. J. Stott, Ultralight bosonic field mass bounds from astrophysical black hole spin. arXiv: 2009.07206(2020).https://arxiv.org/abs/2009.07206.
30. P. Fadeev, Y. V. Stadnik, F. Ficek, M. G. Kozlov, V. V. Flambaum, D. Budker, Revisiting spin-dependent forces mediated by new bosons: Potentials in the coordinate-space representation for macroscopic-and atomic-scale experiments. *Phys. Rev. A* **99**, 022113 (2019).
31. D. Budker, P. W. Graham, M. Ledbetter, S. Rajendran, A. O. Sushkov, Proposal for a cosmic axion spin precession experiment (CASPEr). *Phys. Rev. X* **4**, 021030 (2014).
32. K. Kaneta, H.-S. Lee, S. Yun, Portal connecting dark photons and axions. *Phys. Rev. Lett.* **118**, 101802 (2017).
33. T. Kornack, S. Smullin, S.-K. Lee, M. Romalis, A low-noise ferrite magnetic shield. *Appl. Phys. Lett.* **90**, 223501 (2007).
34. I. Kominis, T. Kornack, J. Allred, M. V. Romalis, A subfemtotesla multichannel atomic magnetometer. *Nature* **422**, 596–599 (2003).
35. V. M. Acosta, E. Bauch, M. P. Ledbetter, C. Santori, K. M. C. Fu, P. E. Barclay, R. G. Beausoleil, H. Linget, J. F. Roch, F. Treussart, S. Chemerisov, W. Gawlik, D. Budker, Diamonds with a high density of nitrogen-vacancy centers for magnetometry applications. *Phys. Rev. B* **80**, 115202 (2009).
36. J. M. Schloss, J. F. Barry, M. J. Turner, R. L. Walsworth, Simultaneous broadband vector magnetometry using solid-state spins. *Phys. Rev. Appl.* **10**, 034044 (2018).
37. H. Wu, S. Mirkhanov, W. Ng, K. C. Chen, Y. Xiong, M. Oxborrow, Invasive optical pumping for room-temperature masers, time-resolved EPR, triplet-DNP, and quantum engines exploiting strong coupling. *Opt. Express* **28**, 29691–29702 (2020).
38. K. Tateishi, M. Negoro, S. Nishida, A. Kagawa, Y. Morita, M. Kitagawa, Room temperature hyperpolarization of nuclear spins in bulk. *Proc. Natl. Acad. Sci. U.S.A.* **111**, 7527–7530 (2014).
39. C. S. Wood, S. C. Bennett, D. Cho, B. P. Masterson, J. L. Roberts, C. E. Tanner, C. E. Wieman, Measurement of parity nonconservation and an anapole moment in cesium. *Science* **275**, 1759–1763 (1997).

Acknowledgments: We thank V. Flambaum, H. Wu, D. Sheng, Y. Cai, and Y. Chen for valuable discussions. **Funding:** This work was supported by National Key Research and Development Program of China (grant no. 2018YFA0306600), National Natural Science Foundation of China (grants nos. 11661161018, 11927811, and 12004371), Anhui Initiative in Quantum Information Technologies (grant no. AHY050000), USTC Research Funds of the Double First-Class Initiative (grant no. YD3540002002), and the Deutsche Forschungsgemeinschaft (DFG) Project ID 423116110. This work was also supported by the Cluster of Excellence "Precision Physics, Fundamental Interactions, and Structure of Matter" (PRISMA+ EXC 2118/1) funded by the German Research Foundation (DFG) within the German Excellence Strategy (Project ID 39083149). **Author contributions:** Y.W. and Y.H. designed the experimental protocols, performed the experiments, analyzed the data, and wrote the manuscript. C.G., X.K., and Y.Q. performed the experiments and edited the manuscript. H.S., W.J., and D.H. analyzed the data and edited the manuscript. M.J., X.P., and D.B. proposed the experimental concept, designed the experimental protocols, and proofread and edited the manuscript. All authors contributed with the discussions and checking of the manuscript. **Competing interests:** The authors declare that they have no competing interests. **Data and materials availability:** All data needed to evaluate the conclusions in the paper are present in the paper and/or the Supplementary Materials.

Submitted 20 July 2022
Accepted 1 December 2022
Published 6 January 2023
10.1126/sciadv.ade0353